




## Synchronization of bowhead whales

Evgeny A. Podolskiy <sup>1,\*</sup>, Jonas Teilmann <sup>2</sup>, and Mads Peter Heide-Jørgensen <sup>3</sup><sup>1</sup>Arctic Research Center, Hokkaido University, 001-0021, Sapporo, Japan<sup>2</sup>Marine Mammal Research, Department of Ecoscience, Aarhus University, DK-4000, Roskilde, Denmark<sup>3</sup>Greenland Institute of Natural Resources, DK-1401, Copenhagen, Denmark

(Received 5 February 2024; accepted 10 July 2024; published 15 August 2024)

Inferring animal behavior from irregular tracking data is a challenging area of research. It is particularly difficult to determine if whales, who intermittently explore different depths while staying in the same acoustic medium, synchronize their days with their prey and each other over kilometer-scale distances. Here, we aim to better understand the diving behavior of bowhead whales (*Balaena mysticetus*) in Disko Bay, West Greenland, using the largest high-frequency dive-depth dataset to date (144 days at 1 Hz from 12 different whales) and nonlinear dynamics, whereby we consider the whales to be chaotic (aperiodic) oscillators. We find that foraging whales dive deeper during the daytime in spring, with this diving behavior being in apparent synchrony with their vertically migrating prey. Furthermore, we demonstrate that bowhead whales can synchronize their behavior with each other for up to a week while staying within a range of up to  $\sim 100$  km. This discovery agrees with the acoustic herd theory of long-range signaling in baleen whales. On the other hand, the synchrony might emerge when animals experience similar ecological conditions, which are, however, difficult to name because targeted depths and locations were separated for hundreds of meters and tens of kilometers, respectively. In this paper, we identify a framework for studying the sociality and behavior of such chaotically moving, unrestrained marine animals and call for more simultaneous tagging campaigns.

DOI: [10.1103/PhysRevResearch.6.033174](https://doi.org/10.1103/PhysRevResearch.6.033174)

## I. INTRODUCTION

The synchronized activities of enormous filtering organisms, such as whales, remain poorly known owing to limited observations and data analysis techniques. Bowhead whales (*Balaena mysticetus*) are among the largest baleen whales (up to 19 m long) and longest-living mammals in the world (individual whales may live for  $>200$  y) [1,2]. Endemic to the Arctic Ocean, they provide an important service to ocean ecosystems via aquatic-microorganism (i.e., zooplankton) consumption ( $\sim 6000$  kg  $d^{-1}$ ), water filtration ( $\sim 60\,000$  m<sup>3</sup>  $d^{-1}$ ), and nutrient recycling [2–4]. Bowhead whales also remain important to northern indigenous communities through subsistence hunting [5]. As the bowhead whale population continues to recover after overexploitation in the 19th century [6], its ecological role is expected to grow; however, climate change, sea-ice loss, and industrial activities will likely have negative impacts [7–9]. Elucidating the behavioral repertoire and sociality of bowhead whales is therefore increasingly important, as pressure from humans, shifts in zooplankton composition, killer whale (*Orcinus orca*)

predation (the risk of which is growing as ice cover decreases), and Arctic warming continue to increase [2,8–11].

Biologging offers a more comprehensive view into the ethology of marine mammals compared with visual observations, as it documents the diel activity patterns and habitat associations of individuals over periods of several days or longer [12]. However, the derivation of behavioral traits from these continuous time-depth records is challenging and often simplified. Bowheads generally forage on zooplankton via a continuous ram filtration (i.e., swimming with an open mouth) and are known to feed in all parts of the water column [13]. Nevertheless, previous bowhead studies have excluded shallow dive data (shallower than 8–20 m depth) from their analysis [7,9,14]. Dives to  $<20$  m depth comprise nearly half of the time budget of the whales in our dataset (Appendix A). The commonly employed logic that deeper U-shaped dives serve as a feeding proxy [9,13] means that the whales in our dataset spent only 11–17 h  $d^{-1}$  for foraging. The rationale for excluding these surface intervals depends on the local bathymetry (i.e., seafloor topography) and pycnocline (i.e., layer with the greatest vertical density gradient) depth that the bowheads are traversing [9,14]. These dive-depth trends may also be population and/or location specific. For example, surface feeding (skim feeding) has not been observed in West Greenland waters, presumably because of the low zooplankton biomass near the surface [14], whereas surface feeding is common in Alaskan waters [2]. Shallow dive depths may therefore be indicative of foraging behavior. Furthermore, concurrent tracking has highlighted a striking shift in the bowhead whale habitat toward sea ice, where killer whales

\*Contact author: [e.podolskiy@arc.hokudai.ac.jp](mailto:e.podolskiy@arc.hokudai.ac.jp)

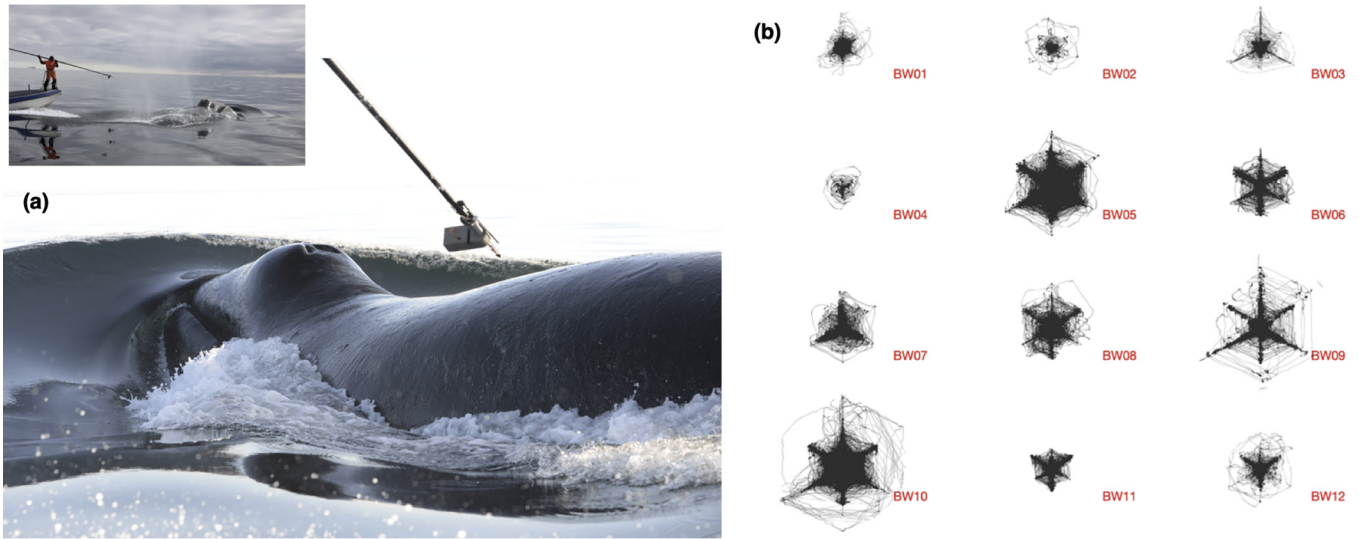


FIG. 1. Bowhead whale behavioral state-space reconstruction. (a) Bowhead whales are first tagged in Disko Bay, West Greenland, to track their movements and diving behavior. Photo credits: M.P. Heide-Jørgensen (2017). (b) The abstract behavioral portrait (state-space) for each of the 12 tagged whales is reconstructed by a time-delay embedding, which is a tool of nonlinear time series analysis. We plot the bowhead whale dive time series value (Fig. 8) against the values taken a delay time  $\tau$  and  $2\tau$  later. This is performed with individually computed delays  $\hat{\tau}_i$  and embedding dimension  $m = 3$ ; for an explanation of this concept and its parameters, see Appendix C.

are present, and has been interpreted as an ice-as-refuge strategy [8]. Regardless of the reason behind this sea-ice-seeking behavior, sea ice may potentially serve as a vertical boundary condition that restricts dive patterns, as suggested for narwhals [15]. These observations and inferences imply that continuous, long-term dive data may be fundamental for quantitatively analyzing the ethology of bowheads and conducting cross-population comparisons among both bowhead populations and other cetaceans. However, the key challenge with such data is the ability to effectively identify specific behaviors from the observed movement data [16].

Oscillating systems are the main subject of nonlinear dynamics. A whale can effectively be viewed as a chaotic self-sustained oscillator (i.e., aperiodic and oscillating without external forcing) that balances its behavior between a need for oxygen (at the surface) and a need for food (at depth). It has been recently shown that narwhal chaotic diving patterns can be quantified via time-delay embedding, which holds key advantages over other methods such as commonly used hidden Markov models owing to its simplicity [15]. Time-delay embedding is a tool to convert a time series into a geometrical object for state-space reconstructions [17–19]. This dynamical systems chaos approach is being increasingly used in quantitative ethology and neuroscience; however, it has been largely limited to neurones and small laboratory organisms such as flies, worms, zebrafish, and mice [20–23]. Such approaches to quantify the spontaneous behavior of unrestrained animals are therefore substantially lagging [24].

Here, we aim to gain insights into the behavior of some of the largest animals on Earth by mapping dive records from instrumented bowhead whales in Disko Bay, West Greenland, onto an abstract state-space framework to reconstruct an individual attractor of each whale. (The term *attractor* is broadly defined as a set to which all neighboring trajec-

tories of a dynamical system converge [25].) Our analysis reveals that bowheads generally stayed closer to the surface at night and dove deeper in the afternoon throughout spring, coincident with the diel vertical migration (DVM) of their principal prey, zooplankton. Also, we show that there is an episodic days-long coupling in the behavior of a whale pair, which corresponds to synchronization between two chaotic oscillators over a kilometer-scale range. We discuss how it fits the acoustic herd theory of long-range signaling [26] and the likelihood of alternative interpretations. Insightful employment of a nonlinear state-space reconstruction highlights that dynamic approaches are indispensable for investigating animal behavior, particularly when observations are limited.

## II. MATERIALS AND METHODS

We compiled  $\sim 144$  d of bowhead whale dive records from 12 tag deployments at a high temporal resolution (1 Hz) from Disko Bay, West Greenland (Appendixes A and B). The following three features make this dataset unique and set apart from the previous literature presenting fine-scale time-depth records of bowhead whales [7,13]: the longest length, the largest sample size, and previously unavailable simultaneous attachment times (see Appendix A for details). Such a rich dataset provides insights into bowhead whale behavior that were previously difficult to obtain via discrete records of maximum depth per dive and similar snapshots that were imposed by archival tag systems and arbitrarily chosen thresholds [7,27,28].

We performed a state-space reconstruction via the time-delay embedding (see Appendix C [15,18]) to better understand the continuous complexity of the diving behavior of each tagged whale. This approach transforms each individual dive record into a three-dimensional flowing geometrical

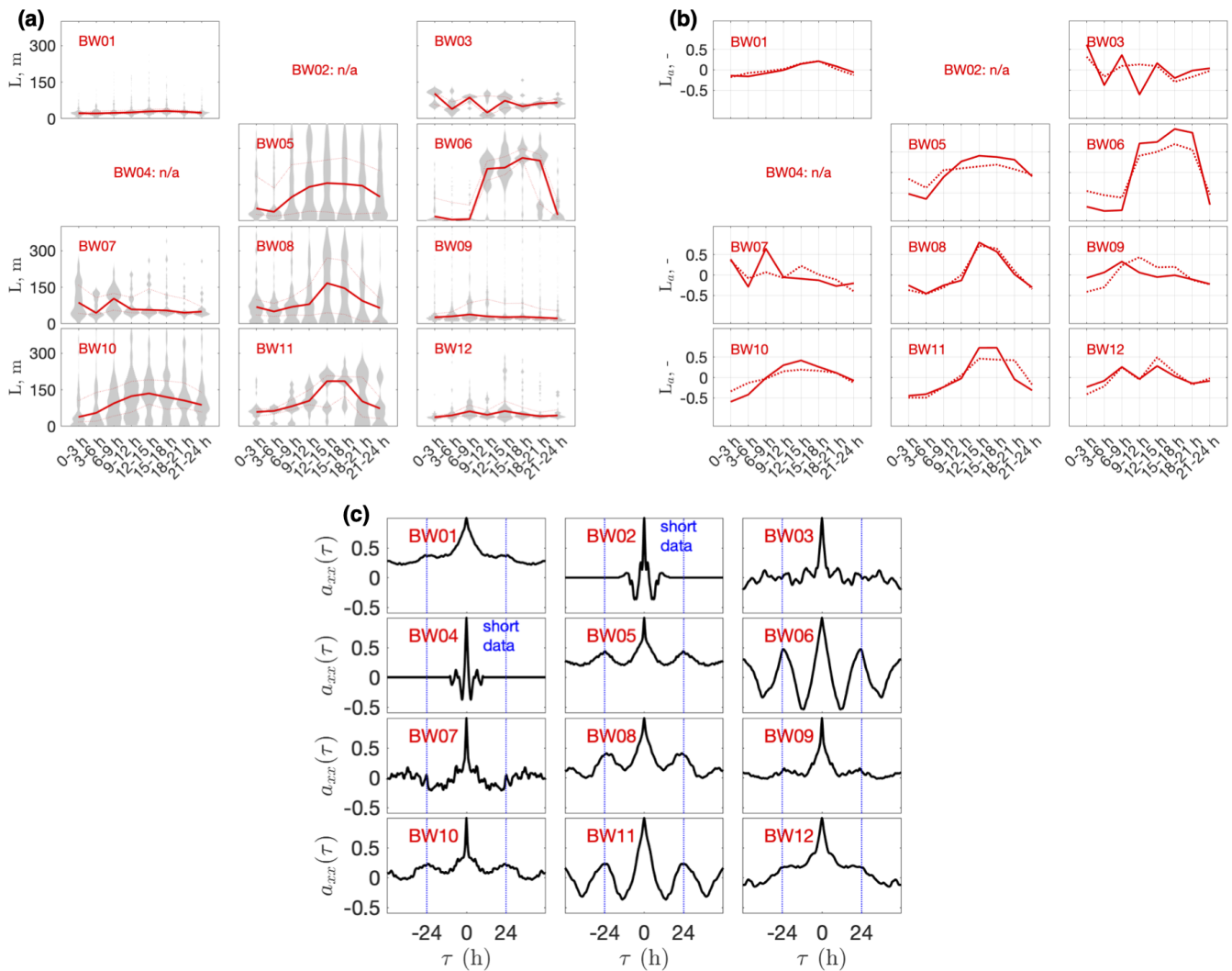


FIG. 2. Euclidian distance over a 24 h cycle for each bowhead whale. (a) Smoothed histograms of Euclidian distance  $L_i$  binned into 3 h intervals during a day. Euclidian distance is a distance between the origin and points in embedding space, which intuitively can be seen as a relative depth targeted by the whale. Only whales with  $>24$  h of dive data are shown. The thick red curve is the median distance, and the lower and upper dashed red curves correspond to the 25th and 75th percentiles, respectively. (b) Associated anomalies relative to the mean value  $[L_a = \frac{L(i) - \bar{L}}{\bar{L}}]$ , which are computed for the median (solid curve) and the 75th percentile (dash curve). (c) Autocorrelation functions  $a_{xx}(\tau)$  of the Euclidian distances (demeaned and smoothed using a median filter with a 1 h window size), which are computed for lags  $\tau$  up to 48 h.

structure called a strange attractor (Fig. 1). The behavioral state-space reveals the orbital nature of the dive data and shows how recurrent trajectories separate outward for deeper diving bouts and approach the origin for shallow dives [15].

### III. RESULTS AND DISCUSSION

#### A. Diel rhythm

Here, we characterize variability of bowhead whale behavior (Fig. 1), by computing a basic chaotic invariant of the Euclidian distance between the origin and each point of the state-space and then analyzing its temporal dynamics [15]. At least half of the whales exhibited a similar diel behavior pattern throughout spring (March–May), with greater depths achieved in the afternoon (Fig. 2). This is clearly observed for whales BW01, BW05, BW06, BW08, BW10, and BW11 [the median agrees with the 75th percentile (P75)] but is less obvious for whales BW07, BW09, and BW12. Independent

verification via an autocorrelation function (Fig. 2) confirms the presence of a diel pattern of diving behavior in all whales that possess  $>24$  h of dive data, with the exception of whale BW03. This analysis collectively shows that at least 8 of the 12 tagged whales exhibited a diel diving behavior.

A previous analysis of maximum dive depths showed that eight instrumented bowhead whales in Cumberland Sound, East Canada ( $\sim 3.5^\circ$  south of Disko Bay), performed deeper diving bouts during the daytime in August 2012 [27]. However, a follow-up study of nine tagged bowhead whales in the same region in August–September 2016 found no evidence of diel diving behavior [7]. A study of six bowhead whales in the Chukchi Sea (between Siberia and Alaska, at a similar latitude to Disko Bay) also found no evidence for a diel diving behavior in autumn [29]. Regardless, modeling studies have proceeded with major assumptions [3], even though the existence of day-night behavioral differences is inconclusive. A key assumption is that the feeding rate

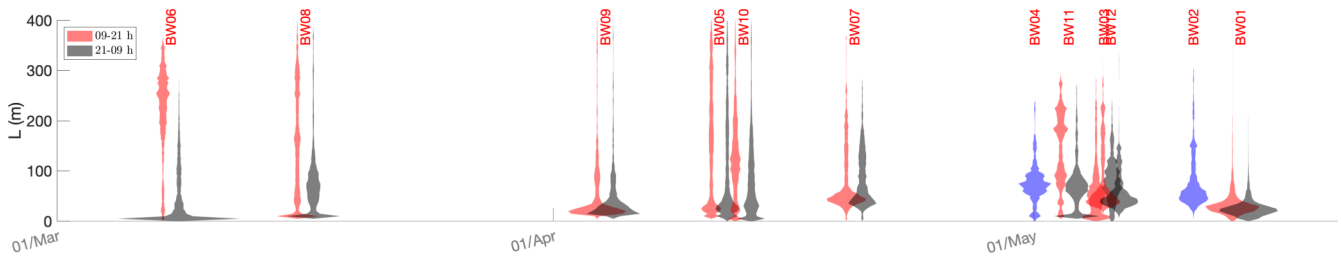


FIG. 3. Euclidian distance statistics for the 12 tagged whales. Histograms of the Euclidian distance  $L_i$  are plotted for the mean day of the deployment year (asynchronous, 2008–2018). For an explanation of  $L_i$ , see the caption of Fig. 2 and Appendix C. Red and gray shadings are indicative of daytime (09–21 h) and nighttime (21–09 h) movements, respectively. Blue shading indicates  $<24$  h data and has been plotted unseparated (whales BW02 and BW04). The original data are provided in Fig. 4. Figure 5 has zoomed-in portions of the figure for showing the differences between the early and late spring.

estimation requires segmentation of the behavior into daytime and nighttime phases to minimize the errors in annual prey consumption. For example, it has been assumed that the northeast Pacific blue whale (*Balaenoptera musculus*) has low feeding rates in temperate feeding grounds at night and that balaenids (including bowhead whales) only feed during the day, such that 10 and 15 h could be taken as low and high foraging efforts per day, respectively [3].

The most likely cause of diel diving behavior might be the DVM of the principal prey of the bowhead whale, *Calanus* [27]. DVM is strongest in fall and spring in the Arctic, with zooplankton retreating into deeper waters during the daytime and returning to shallow depths around midnight, even under the midnight sun (24 h of daylight) [30,31]. The same phenomenon likely provides nocturnal near-surface foraging opportunities to sea birds breeding in West Greenland [32]. Similarly, more blue-whale calls were observed in low-latitude breeding grounds during the dark and dusk periods, when krill (exhibiting DVM) were near the surface [33]. It has been suggested that blue whales forage mostly at depth during the day and stay near the surface at night while tracking the vertical migration of their prey [33,34]. Moreover, physiological constraints [35] or high energy expenditure for foraging at depth [12] may make sound production at depth costly [33].

### B. Long-term behavior

Here, we assume that the seasonal behavior of bowhead whales is similar from year to year and plot our Euclidian distance data for the mean day of a corresponding tagging campaign, irrespectively of year (Fig. 3). This visualization of the statistical data confirms previously reported features and reveals trends, as follows.

First, there is some interindividual variability among whales (median Euclidean distance  $=72 \pm 35$  m), which is consistent with the knowledge that bowheads alter their behavior relative to the vertical distribution of their prey biomass [7,9,14,28].

Second, larger Euclidean distances (i.e., deeper diving bouts) become rare toward the end of spring (Figs. 4 and 5). This is expected due to the ontogenetic seasonal vertical migration of *Calanus* [9,14], which is tightly controlled by the local sea-ice coverage and phytoplankton bloom [31].

Third, this late-spring reduction in deeper diving bouts is driven primarily by daytime dives (Fig. 5), with the highest day-night contrast being observed in early spring (see the dive data for whales BW06 and BW08 in Fig. 3; note how the tails in the other dive data either thin or disappear toward the end of spring). This parallels the day-night illuminance difference, which is higher in early spring and weakens toward midsummer, thereby reducing the amplitudes of the expected biorhythms.

Fourth, the time variations in the Euclidean distance for each whale  $L_i$  (Fig. 4) further highlight the presence of a diel cycle and variability in the time commitment to deep diving bouts. The diving bouts are epochs of prolonged separation of the state-space that orbit away from the origin [15]. Such bouts often exceeded 12 h (e.g., in the beginning of April, whale BW05 had marathon bouts lasting  $\sim 14 \pm 4$  h with a brief postmidnight/dusk pause near/at the surface).

Finally, diving bouts seem to start rather abruptly (i.e., steplike) in the beginning of spring and then gradually change their overall shape by the end of April (Fig. 4). The former behavior would be expected when the bowheads are targeting particular prey layers, whereas the latter behavior is likely indicative of bowheads passing through dispersed prey.

Our findings thus far demonstrate that (i) bowhead whales exhibit a diel diving behavior during the spring months in Disko Bay, and (ii) they tend to undertake deeper daytime dives [i.e., between 09:00 and 21:00 local time (LT; UTC-2 h)]. A diel cycle is observed even for those whales that remained relatively close to the surface during late spring (e.g., whale BW01 remained at median depths of  $\sim 13$  m), when their prey is likely to undergo ascension toward the upper layers of the water column [28]. The generally short duration of high-frequency tag attachments (e.g.,  $\sim 3$ –16 h [7,13,28]) means that any conclusions on foraging strategy may be biased based on the season and time of day (e.g., the dive behavior of whale BW06 may appear bimodal on a 24 h scale, but monomodal on a 12 h scale; Fig. 3).

We have established that our self-sustained oscillators have close natural frequencies. Therefore, we will now discuss whether our oscillators can synchronize due to interaction with each other via an acoustic field or under external forcing [36].

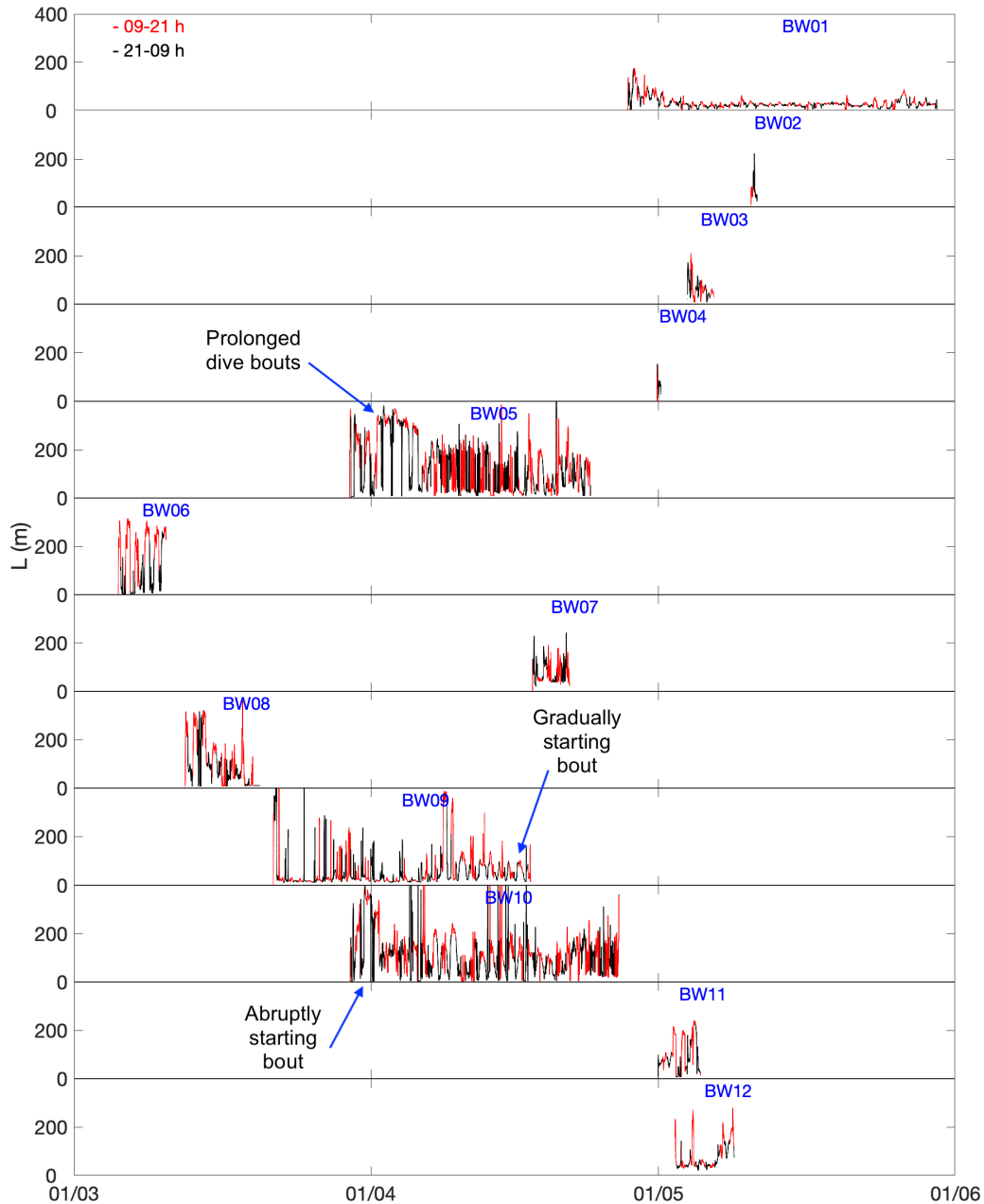


FIG. 4. Time variation of the Euclidian distances. The Euclidian distance for each whale  $L_i$  corresponds to the absolute distance between each point of the state-space and the origin  $[0, 0, 0]$ . When whale  $i$  engages in deep diving bouts, the cyclic trajectories separate further from the origin, and  $L_i$  increases.  $L_i$  is plotted by the day of year (asynchronous, 2008–2018; smoothed using a median filter with a 1 h window). Red curves correspond to the daytime  $L_i$  (09–21 h), and black curves correspond to the nighttime  $L_i$  (21–09 h). Labeled arrows mark the diving bout features that are discussed in the main text.

**C. Chaotic synchronization**

Whales BW05 (female) and BW10 (sex unknown) were spatially separated by 5–352 km during a period of simultaneous observations in April 2010 (Appendix B). Nevertheless, we detected synchronization in their behavior via a classic and straightforward dynamical systems technique (see Appendix D). Specifically, we plotted the phase difference  $\Delta\phi$  of the Euclidian distances  $L_i$  vs time and found two horizontal plateaus, which implies that the whales were episodically locked in their phases (Fig. 6). This synchronization was observed over a quasi-diurnal time scale that lasted up to a week

at a time (an example of a stable constant phase difference is provided in Fig. 7).

The  $L_i$  amplitudes were only weakly correlated, which implies that the whales focused their attention on different depths [Fig. 6(a)]. This is in line with our earlier results (Fig. 3) and the previous suggestion that bowheads demonstrate substantial variability in dive depth, presumably owing to individual foraging strategies and the vertical distribution of prey [27].

In physics, this synchrony is termed an imperfect phase synchronization [37]. The most prominent burst of asynchronous behavior took place during 8–19 April 2010, when

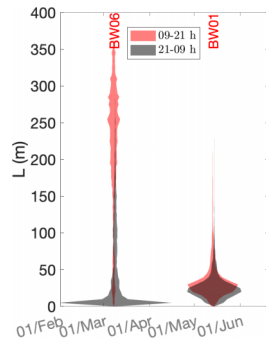


FIG. 5. Euclidian distance statistics for whales BW06 and BW01. Histograms of the Euclidian distance  $L_i$  are plotted for the mean day of the deployment year (asynchronous, 2008 and 2010). Red and gray shadings are indicative of daytime (09–21 h) and nighttime (21–09 h) movements, respectively. The original data are provided in Fig. 4.

whale BW05 temporarily departed Disko Bay to the north [14], while whale BW10 continued its 24 h dive cycle in Disko Bay (Fig. 6). The phase difference was changing continuously and nonuniformly in this desynchronization region, with

nearly constant epochs and rapid phase slips. These intermittent phase-difference dynamics persisted when the distance between whales BW05 and BW10 exceeded the maximum acoustic communication range of bowhead whales ( $\sim 130$  km [38]). This nonstationarity gives an indirect indication in favor of the hypothesized interaction and suggests that our results are unlikely to occur due to the occasional coincidence of frequencies.

We suggest two alternative (but compatible) interpretations on the emergence of such synchrony between two self-sustained oscillators.

First, the whales were coupled via feeding opportunities in the bay. This corresponds to unidirectional entrainment by an external force [i.e., the diurnal cycle imposed by the sun (illuminance) on the ecosystem]. Whale BW05 temporarily disengaged into a different traveling behavior (8 April 2010) and did not encounter prey agglomerations worth targeting, before returning to approximately the same area (19 April 2010) and resuming feeding activities (Appendix B).

Second, the whales were interacting since they could hear each other’s calls (i.e., oscillator entrainment via a sequence of pulses). These interactions remotely mimic those observed in classic mutual synchronization phenomena: a bidirectional

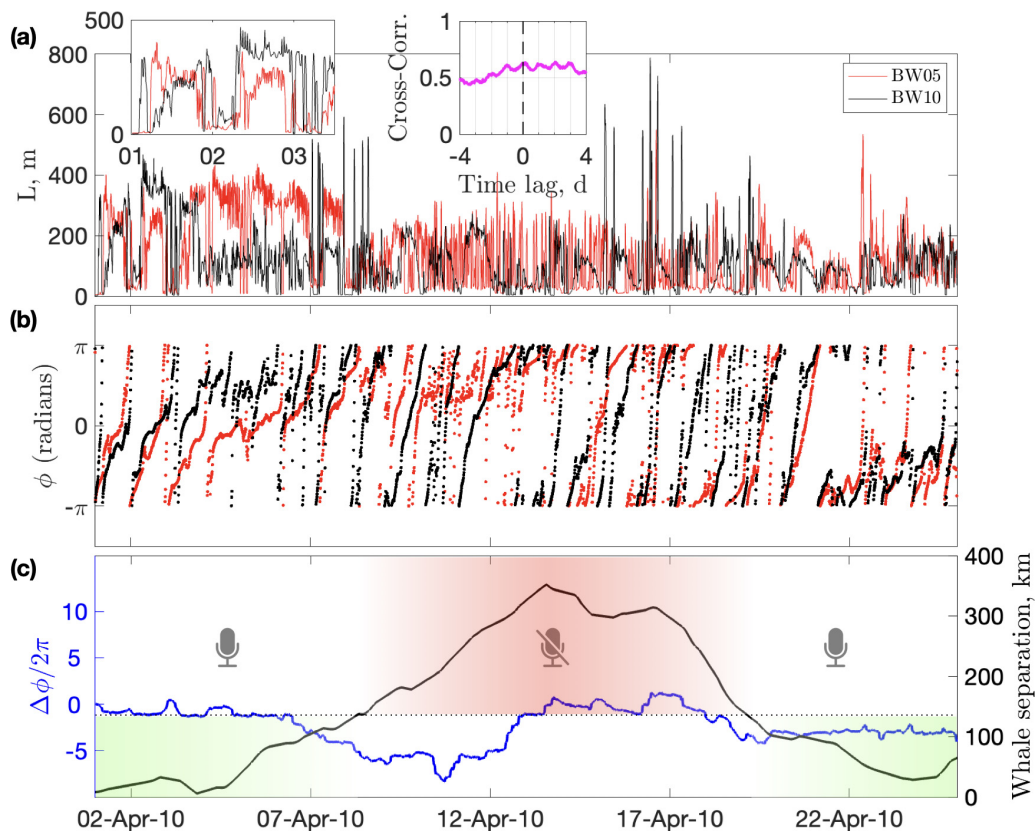


FIG. 6. Episodic synchronization between a whale pair. (a) Covariance of the Euclidian distances  $L_i$  for whales BW05 (red) and BW10 (black). For an explanation of the  $L_i$  see the caption of Fig. 2 and Appendix C. The left inset plot zooms into the first 2.5 d of  $L_i$ . The right inset plot shows the cross-correlation coefficients (magenta curve) between the Euclidian distances, with a clear diel cycle identified. (b) Comparison of the phase angles  $\phi_i$  that are obtained by a Hilbert transform of the Euclidian distances (Appendix D provides details on this signal-processing technique). (c) Corresponding phase difference  $\Delta\phi$ , which is derived from the unwrapped phase angles [the process of unwrapping removes the  $2\pi$  jumps that are present in (b)]. The main episodes of phase locking (where  $\Delta\phi$  is very small and fluctuates around a constant) take place when the whales remain within the maximum acoustic communication range of  $\sim 130$  km [38] (black line; green/red shading indicates where the acoustic contact is likely/unlikely).

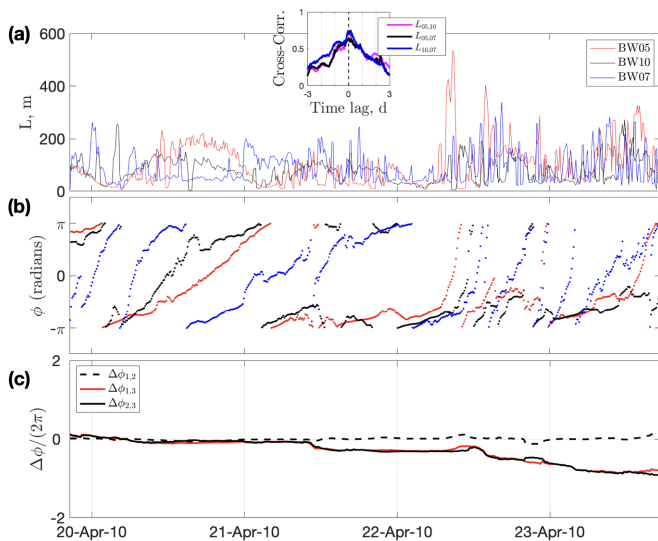


FIG. 7. Synchronization results between whale pairs in April 2010. (a) Euclidian distances of whales BW05 (red), BW07 (blue), and BW10 (black). The inset plot shows the cross-correlations between the Euclidian distance pairs. (b) Comparison of the phase angles  $\phi_L$ , obtained via a Hilbert transform of the Euclidian distances. (c) Corresponding difference  $\Delta\phi$  of the unwrapped phases for each whale pair [BW05 vs BW10 (dashed), BW05 vs BW07 (red), and BW10 vs BW07(black)].

adjustment of oscillator rhythms due to their weak interactions (e.g., pendulum clocks, violinists, applause, fireflies) [36]. We note that this interaction may be similar to that of foraging blue whales, who produce significantly more frequency-modulated moans (B call) at night when they are near ( $\sim 30$  m) the surface, with these interactions possibly linking the behavior of individual whales [33,34].

However, basic biological observations that may support these hypotheses are limited and often focus on surface behavior. Quantitative evidence has only been reported for synchronous surface behavior (e.g., the breathing of pilot whales [39]) and is usually constrained to nonsystematic visual observations [40]. Würsig and Koski [2] highlighted that a synchrony in the surfacings and dives of bowhead

whales (e.g., feeding bouts of 0.5 h duration in echelon formation) is a widespread and frequent observation, at least in Alaska, that has yet to undergo rigorous analysis and that surface-dive cycles have been witnessed, even among widely dispersed bowheads. However, the large distances between these two whales, the low correlation of their Euclidian distances ( $L_{BW05,BW10}$ ), and the time scale of phase locking indicate that the synchrony was not the spatially synchronized arbitrary motion one would expect [e.g., sexual interactions, mother-calf interactions, or feeding in close proximity (i.e., in echelon formation)]. Furthermore, prey-ingestion coordination is unlikely for bowheads feeding on slow-swimming copepods [2].

An alternative explanation might be the preservation of acoustic communication for various socializing purposes (including avoidance of killer-whale predation [10], as expressed in detail in Refs. [2,41]). For example, the aforementioned associative link between the calling and diving behavior of blue whales was interpreted in terms of foraging [33] but within a range herd theory [26]. The latter refers to a social structure of whales held together by long-range acoustic signaling, which might optimize the search for prey, facilitate migration, and increase rendezvous/reproductive opportunities [26,33]. Distributed-array observations in Alaska have shown that at least two bowhead whales individually exchanged stereotypical calls for hours with remarkable synchrony while swimming along tracks separated by  $\sim 2.5$  km [42]. This isolated observation suggests that bowheads may maintain the cohesion of their acoustic herd during springtime migrations by signature calls (Refs. [42,43] and references therein).

The observed behavior might also be similar to that of long-finned pilot whales, as group members generally do not synchronize individual dives but do synchronize diving bouts [40]. However, we hesitate to extend our findings to a group because we were unable to clearly detect synchronization that persisted longer than a day or so in another three cases. The only other whale that was tagged in April 2010, BW07 (male; range unknown), was possibly synchronized to whales BW05 and BW10 but only for a brief period of  $< 1$  d (Appendix D). Simultaneous data were available for only two whales in May 2018 (BW11 and BW12 at unknown range; it is only known

TABLE I. Depth records from the 12 tagged bowhead whales in Disko Bay, West Greenland (2008–2018). See Supplemental Material [46] for data files.

Whale	Sex	Instrument	S/N	File name
BW01	F	Phyllis_2008	08A0189	Phyllis2008.csv
BW02	F	Elise_2009	08A0045	08A0045_Elise2009.csv
BW03	M	Phyllis_2009	08A0189	08A0189.csv
BW04	F	Tove_2009	09A0022	09A0022_Tove2009.csv
BW05	F	Elise_2010	08A0045	08A0045_ELISE.csv
BW06	n/a	Birgit1_2010	09A0042	09A0042_BIRGIT.csv
BW07	M	Birgit2_2010	09A0042	09A0042_BIRGIT2_2010.csv
BW08	n/a	Tove_2010	09A0022	09A0022_TOVE.csv
BW09	n/a	Elise_2011	08A0045	ELISE_2011.csv
BW10	n/a	Phyllis_2010	08A0189	08A0189 Retrieved 15Oct2014.csv
BW11	n/a	60022-2018	09A0788	60022_09A0788_2_Dive data_GPS_OK.csv
BW12	n/a	BW12-2018	09A0905	BW12_2018.csv

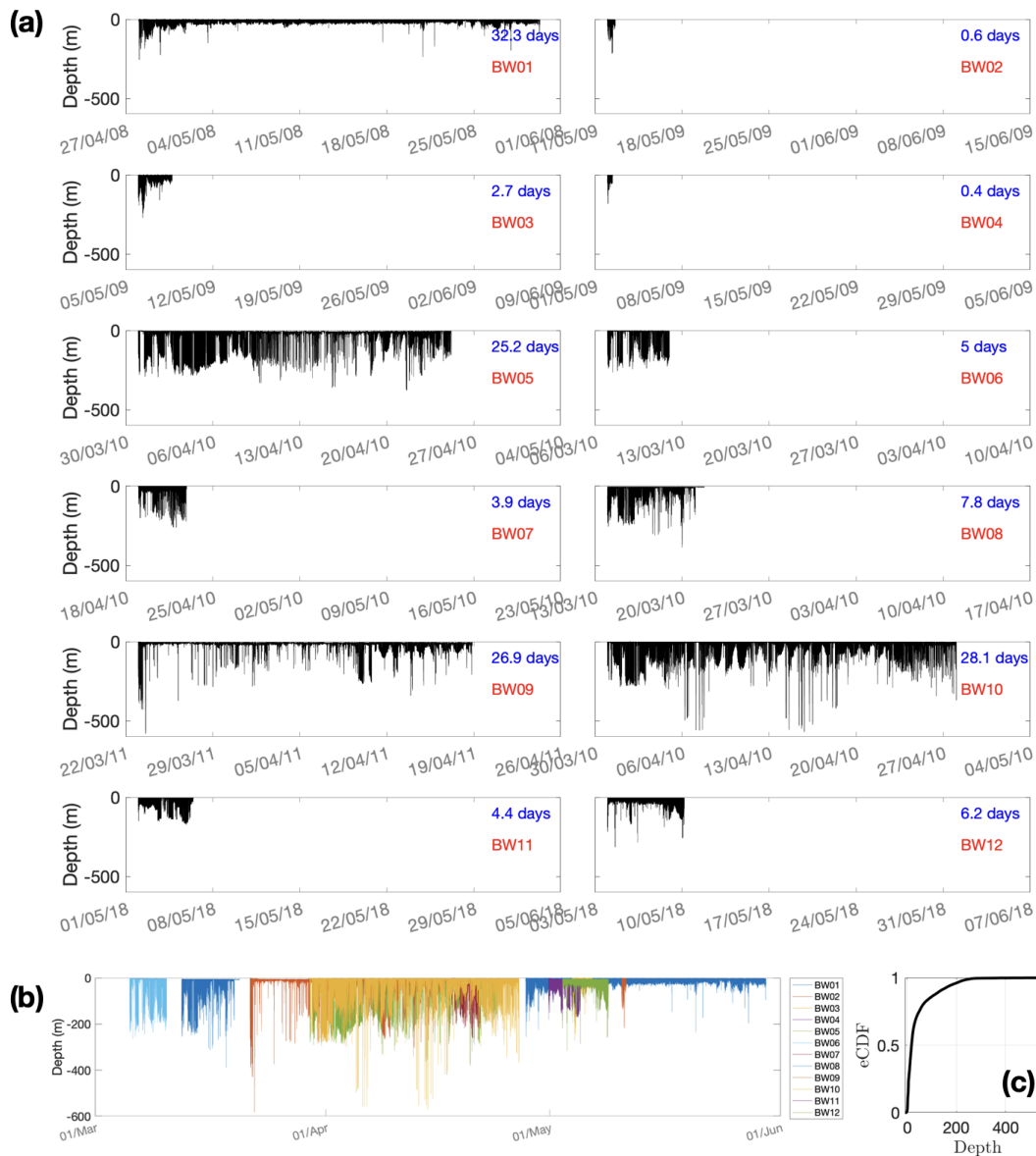


FIG. 8. Depth records from the 12 tagged bowhead whales in Disko Bay, West Greenland. (a) Individual data for each tagged whale. (b) All data relative to the start of a year, irrespectively of year (asynchronous). (c) Empirical cumulative distribution function for all depth data.

that whale BW11 stayed in Disko Bay), but the dataset was too short, and the phase difference changed in an intermittent fashion (Appendix D). The lack of a clearly synchronous state (Appendix D) works against the aforementioned case of external forcing. Furthermore, we can also expect some partially synchronous states when several whales form clusters of synchronized elements, whereas their neighbors have their own frequencies, as observed in laser arrays, where the interaction depends on the distance [36].

Without direct evidence, such as recordings made of the two whales, it is not possible to determine that the individuals were in acoustic contact. However, this issue is difficult to address due to limitations of currently available field approaches, such as the use of digital acoustic tags (DTAGs). It is challenging owing to (i) a short recording duration (<24 h; i.e., insufficient to document the separation of whales for tens to hundreds of kilometers), and (ii) a drift of internal clocks,

making precise association of exchanged calls traveling for more than 10–60 s (and thus proving the causality) difficult.

#### IV. CONCLUSIONS

Our results demonstrate the following. First, chaos approach is an efficient tool for uncovering hidden information within the apparently disorderly collective behavior of large marine animals, such as whales. Until recently, state-space reconstructions in quantitative ethology have been biased toward small animals (e.g., [22]) or just one individual narwhal [15]. Second, bowhead whales in Disko Bay exhibit a diel diving behavior in spring and usually dive deeper in the afternoon, presumably tracking the DVM of zooplankton. Until now, this has not been shown for spring and remained contradictory for autumn [7,27,29]. Third, our data reveal a long-distance affiliative relationship between a pair of bow-



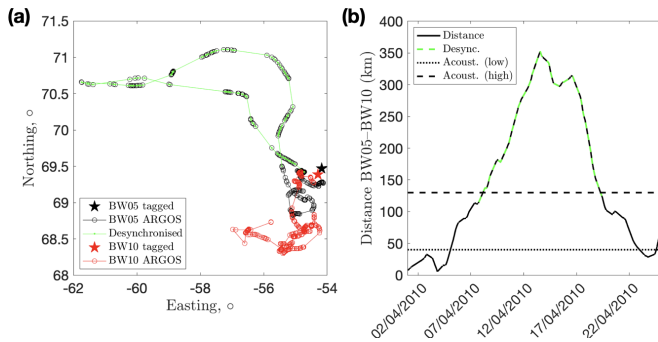


FIG. 9. Locations of two whales relative to each other. (a) Initial tagging locations (stars) and ARGOS-derived locations for whales BW05 (black) and BW10 (red). The green line marks the time of the most prominent desynchronization epoch (8–19 April 2010; see the main text and Fig. 6 for further details). (b) Distance between whales BW05 and BW10 during the period when they were simultaneously monitored. Dashed horizontal lines show the lower (40 km) and upper (130 km) estimates of the bowhead whale acoustic communication range in Disko Bay [38].

head whales (or rephrasing Huygens [36], the sympathy of two whales) with the behavioral repertoire of bowhead whales possibly including synchronization over periods of several days or longer. Despite reports from several hundred tag deployments in the literature to date [3] and a belief that bowheads are some of the best-studied cetaceans, whale-pair diving synchronization has not been revealed from depth records until now.

Given the limited nature of the data, we suggest that bowheads are embedded into an oscillatory medium of foraging opportunities that entrains them into a diel rhythm and that they may try to match to each other’s behavior acoustically over long distances (for the facilitation of predator avoidance [2,10,41], reinforcement of social bonds, and effective foraging), as not doing so would be evolutionary disadvantageous [26]. We suggest that the range herd theory [26] is the most plausible interpretation. An alternative explanation is that the two animals were experiencing similar ecological conditions [44]. However, it is difficult to identify such conditions, persistent for up to a week, for animals exploring depths and locations which were different for hundreds of meters and tens of kilometers, respectively, especially when three simultaneous record pairs did not yield clear synchronization. Explanation of Huygens synchronization of two clocks took 350 years [45], and it would be naïve to hope to explain the synchronization of whales within just one study. Therefore, we call for more simultaneous tag deployments for further evidence.

Given that the social structures of bowhead whales and other cetaceans remain poorly known [39] and their role in marine ecosystems continues to increase in a rapidly changing environment [3], nonlinear dynamics can serve as a powerful approach for investigating their diving behavior and sociality.

The data reported in this paper are available in the Supplemental Material [46] and in Ref. [14]. The MATLAB code used in this paper is openly available via Ref. [15].

## ACKNOWLEDGMENTS

This paper was funded by the Commission for Scientific Research in Greenland, the National Ocean Partnership Program, the Office of Naval Research, and the Greenland Institute of Natural Resources. E.A.P. thanks the Arctic Challenge for Sustainability II research project (ArCS-II; No. JPMXD1420318865), Grants-in-Aid for Scientific Research (KAKENHI, No. 24K02093), and Hokkaido University for support. The bowhead whale tagging was permitted by the Government of Greenland to the Greenland Institute of Natural Resources. The authors thank the three anonymous reviewers for their comments on the initial version of this paper.

## APPENDIX A: DIVE-DEPTH RECORDS

Time-depth records were collected for 12 bowhead whales in Disko Bay, West Greenland, using archival tags that measured the water depth at a 1 Hz sample rate, providing 0.5 m resolution. These instrumented whales belong to the East Canada–West Greenland population; they remain in Disko Bay—their wintering ground and spring feeding area, until early June, when the sea ice recedes and the surface water temperature rises [47]. The procedure for bowhead whale depth collection is detailed in Ref. [14]. The dive data that are analyzed in this paper are listed in Table I and visualized in Fig. 8. The data include nine whales BW01–BW09 (2008–2011), which are partially described in Ref. [14], and appended with three whales BW10–BW12 (2010 and 2018). We note, however, that even if nine of these tag deployments were originally presented in Ref. [14], none of our key findings overlap.

Each record was visually inspected to remove obvious periods when a tag was detached from the whale. Therefore, there may be slight differences in the stated record durations of Ref. [14] and this study. We also assume that the behavioral perturbation by tagging had a negligible effect on the diving profiles, as the characteristic recovery time in bowheads is much shorter (<9 h [48]) than the duration of most records (with the exception of the BW02 and BW04 records). We refer to the local time (LT; UTC–2 h) throughout the paper. The deepest dive of the dataset ~582 m was made by whale BW09; however, 99% of the dives by all of the whales were shallower than 250 m [Fig. 8(c)].

Overall, to our knowledge, the sample size ( $n = 12$ ) is the largest in the literature analyzing fine-scale data of bowhead whales. For example, previous studies analyzed  $n = 3$  animals with undisturbed diving behavior recorded for <15.6 h [7], or  $n = 7$ , but with attachment time not exceeding 3 h [13], which is shorter than the characteristic recovery time in bowheads [48].

## APPENDIX B: LOCATIONS

We followed the recalculation method of Ref. [49] to obtain reliable whale locations from ARGOS satellite tracking measurements (Fig. 9).

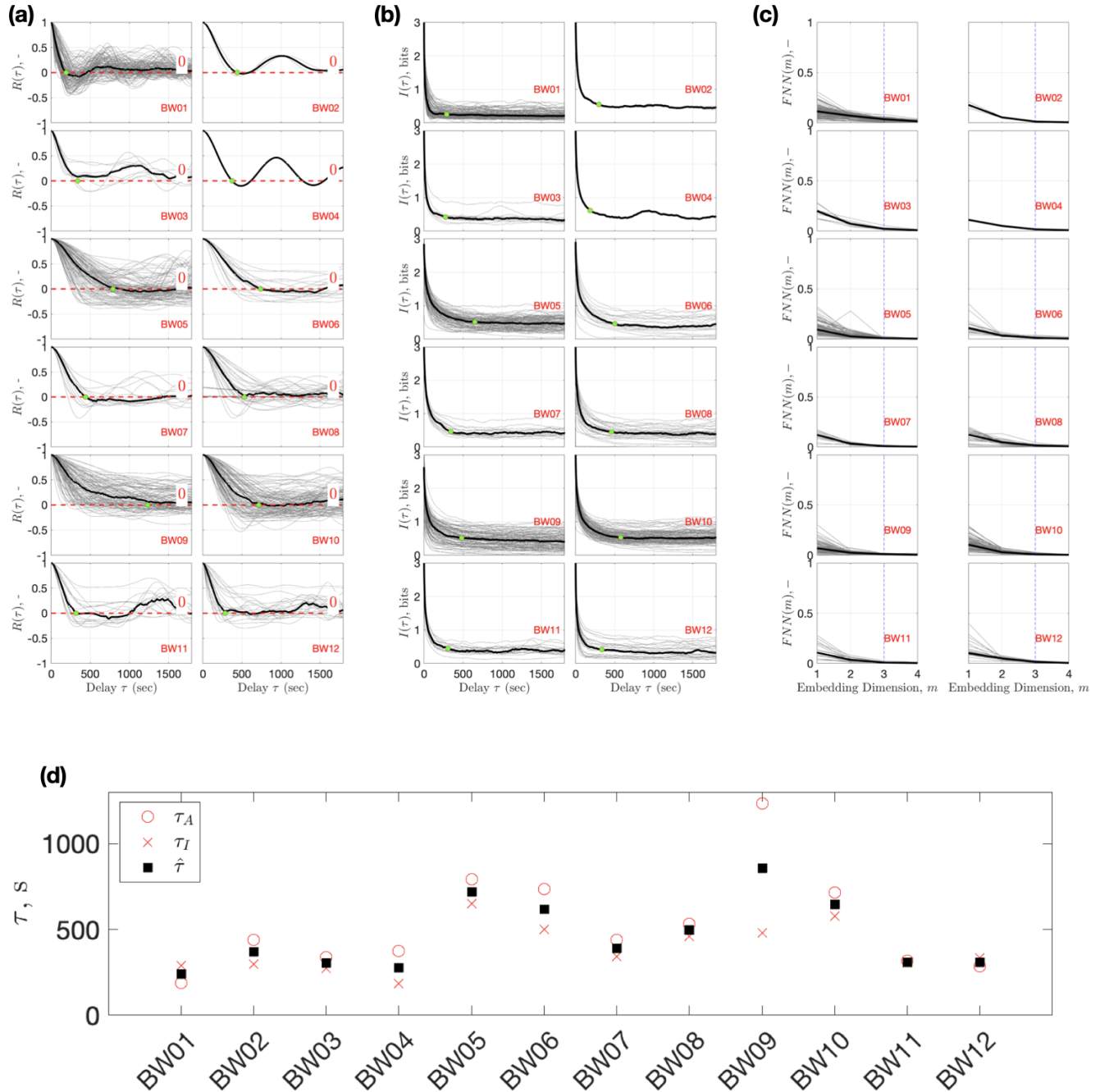


FIG. 10. Self-similarity time scales and false-negative neighbors for each dive record. (a) Autocorrelation (green circles indicate the estimated decorrelation time  $\tau_A$ ). (b) Self-mutual information (green circles indicate the information loss time  $\tau_I$ ). (c) False-negative neighbors (FNN; estimated for the  $\tau$  values shown in (d) and corresponding to the individual self-similarity time  $\hat{\tau} = \frac{\tau_A + \tau_I}{2}$  and  $r = 3$ ). (d) Delay times  $\tau$  for each tagged whale. All statistical features were computed using 6-h-long nonoverlapping segments, with the global median values shown in black. Dashed vertical lines in the FNN plots show that the number of false neighbors is reasonably low when  $m = 3$ .

**APPENDIX C: TIME-DELAY EMBEDDING**

We followed the procedure in Ref. [15] to reconstruct the state-space manifold from the dive records via time-delay embedding [18]. The following steps were performed to estimate the optimal delay  $\tau$  and dimension  $m$  embedding parameters using 6-h-long time segments of data (Fig. 10):

(1) Compute the median autocorrelation, and extract the first nearest to zero-crossing delay  $\tau_A$ .

(2) Compute the median self-mutual information and extract the first change in slope  $\tau_I$ .

(3) Take the average ( $\hat{\tau}_i = \frac{\tau_A + \tau_I}{2}$ ) to obtain a compromise value for the time lag, which represents the characteristic decorrelation time scale (Fig. 10). This yielded  $\hat{\tau} = 462 \pm 202$  s (mean  $\pm$  standard deviation).

(4) Compute the false nearest neighbors using  $\hat{\tau}_i$  and  $r = 3$  to confirm that the embedding dimension ( $m = 3$ ) is appropriate, as expected for a free-diving whale [15].

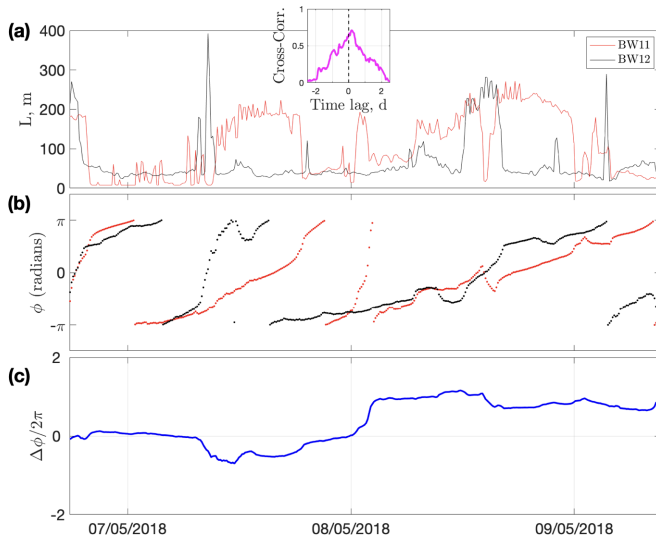


FIG. 11. Synchronization results between a whale pair in May 2018. (a) Euclidian distances of whales BW11 and BW12. The inset plot shows the cross-correlation coefficients between the Euclidian distances. (b) Comparison of the phase angles  $\phi_{L_i}$  obtained via a Hilbert transform of the Euclidian distances. (c) Corresponding difference  $\Delta\phi$  of the unwrapped phases.

(5) Perform time-delay embedding reconstruction with a unique delay  $\hat{\tau}_i$  for each whale in three dimensions ( $m = 3$ ).

The autocorrelation and self-mutual information generally yielded similar estimates of the decorrelation time scale, with the exception of whale BW09 (Fig. 10). We also tested embeddings with higher  $\tau_A$  and lower  $\tau_I$  values for whale BW09, but this had no impact on the key findings of this paper (e.g., the diurnal variation statistics remain unchanged). We note that the autocorrelation and self-mutual information are the most standard techniques for choosing the embedding lag and are

usually sufficient for low-dimensional systems; see Ref. [50] for a comprehensive overview of the existing methods.

We also computed such a measure (or invariant) of the state-space reconstruction as the median Euclidian distance  $L_i$  from the origin (Fig. 4) using a 10 min window [15].

#### APPENDIX D: SYNCHRONIZATION

We investigate for possible synchronization between the chaotic attractors of two or more whales by applying a classic approach based on the Hilbert transform, which allows us to compute the instantaneous phase of an arbitrary nonstationary signal [19,36]. The phase is of pivotal importance for understanding synchronization phenomena, with phase difference analysis being identified as the most straightforward and effective method [36]. Here, we consider Euclidian distance  $L_i$  as a characteristic invariant of each attractor and employ the following procedure to access any potential synchronization among whale pairs.

(1) First, we use a one-dimensional median-filter operator with a 2 h window to reduce the influence of individual dives and demean each  $L_i$  time series.

(2) We then assign phase angles  $\phi_{L_i}$  to the preprocessed data via the Hilbert transform [36]. This yields a time series of time-dependent phase angles (constrained to the  $[-\pi, +\pi]$  interval).

(3) We subsequently unwrap the phases to make them infinitely growing.

(4) Finally, we compute the phase difference  $\Delta\phi = \phi_{L_1} - \phi_{L_2}$  and divide it by  $2\pi$  to express it as the number of complete cycles.

This procedure could only be performed using simultaneously tagged whales: three in April 2010 (BW05, BW07, and BW10), which are shown in Fig. 7, and two in May 2018 (BW11 and BW12), which are shown in Fig. 11. We do not consider a more general form for high-order synchronization ( $|n\phi_{L_1} - m\phi_{L_2}| < \text{constant}$  [36]) because there was the same dominant 24 h cycle in  $L_i$  for most of the tagged whales.

- 
- [1] J. C. George, J. Bada, J. Zeh, L. Scott, S. E. Brown, T. O'Hara, and R. Suydam, Age and growth estimates of bowhead whales (*Balaena mysticetus*) via aspartic acid racemization, *Can. J. Zool.* **77**, 571 (1999).
- [2] B. Würsig and W. Koski, Natural and potentially disturbed behavior of bowhead whales, in *The Bowhead Whale: Balaena Mysticetus: Biology and Human Interactions*, edited by J. George and J. Thewissen (Academic Press/Elsevier, London, 2021), Chap. 23, pp. 339–363.
- [3] M. S. Savoca, M. F. Czapanskiy, S. R. Kahane-Rapport, W. T. Gough, J. A. Fahlbusch, K. C. Bierlich, P. S. Segre, J. Di Clemente, G. S. Penry, D. N. Wiley *et al.*, Baleen whale prey consumption based on high-resolution foraging measurements, *Nature (London)* **599**, 85 (2021).
- [4] L. Gilbert, T. Jeanniard-du Dot, M. Authier, T. Chouvelon, and J. Spitz, Composition of cetacean communities worldwide shapes their contribution to ocean nutrient cycling, *Nat. Commun.* **14**, 5823 (2023).
- [5] R. Suydam and J. George, Current indigenous whaling, in *The Bowhead Whale. Balaena Mysticetus: Biology and Human Interactions*, edited by J. George and J. Thewissen (Academic Press/Elsevier, London, 2021), Chap. 32, pp. 519–535.
- [6] J. W. Higdon, Commercial and subsistence harvests of bowhead whales (*Balaena mysticetus*) in Eastern Canada and West Greenland, *J. Cetacean Res. Manage.* **11**, 185 (2023).
- [7] S. M. E. Fortune, S. H. Ferguson, A. W. Trites, J. M. Hudson, and M. F. Baumgartner, Bowhead whales use two foraging strategies in response to fine-scale differences in zooplankton vertical distribution, *Sci. Rep.* **10**, 20249 (2020).
- [8] C. J. D. Matthews, G. A. Breed, B. LeBlanc, and S. H. Ferguson, Killer whale presence drives bowhead whale selection for sea ice in arctic seascapes of fear, *Proc. Natl. Acad. Sci. USA* **117**, 6590 (2020).
- [9] S. M. E. Fortune, A. W. Trites, V. LeMay, M. F. Baumgartner, and S. H. Ferguson, Year-round foraging across large spatial

- scales suggest that bowhead whales have the potential to adapt to climate change, *Front. Mar. Sci.* **9**, 853525 (2023).
- [10] A. L. Willoughby, M. C. Ferguson, R. Stimmelmayer, J. T. Clarke, and A. A. Brower, Bowhead whale (*Balaena mysticetus*) and killer whale (*Orcinus orca*) co-occurrence in the U.S. Pacific Arctic, 2009–2018: Evidence from bowhead whale carcasses, *Polar Biol.* **43**, 1669 (2020).
- [11] *The Bowhead Whale: Balaena Mysticetus: Biology and Human Interactions*, edited by J. George and J. Thewissen (Academic Press/Elsevier, London, 2021).
- [12] D. A. Croll, A. Acevedo-Gutiérrez, B. R. Tershy, and J. Urbán-Ramírez, The diving behavior of blue and fin whales: Is dive duration shorter than expected based on oxygen stores? *Comp. Biochem. Physiol. A* **129**, 797 (2001).
- [13] M. Simon, M. Johnson, P. Tyack, and P. T. Madsen, Behaviour and kinematics of continuous ram filtration in bowhead whales (*Balaena mysticetus*), *Proc. R. Soc. B* **276**, 3819 (2009).
- [14] M. P. Heide-Jørgensen, K. L. Laidre, N. H. Nielsen, R. G. Hansen, and A. Røstad, Winter and spring diving behavior of bowhead whales relative to prey, *Anim. Biotelemetry* **1**, 15 (2013).
- [15] E. A. Podolskiy and M. P. Heide-Jørgensen, Strange attractor of a narwhal (*Monodon monoceros*), *PLoS Comput. Biol.* **18**, e1010432 (2022).
- [16] A. Roy, S. Lanco Bertrand, and R. Fablet, Deep inference of seabird dives from GPS-only records: Performance and generalization properties, *PLoS Comput. Biol.* **18**, e1009890 (2022).
- [17] N. H. Packard, J. P. Crutchfield, J. D. Farmer, and R. S. Shaw, Geometry from a time series, *Phys. Rev. Lett.* **45**, 712 (1980).
- [18] F. Takens, Detecting strange attractors in turbulence, in *Dynamical Systems and Turbulence, Warwick 1980*, Lecture Notes in Mathematics Vol. 898, edited by D. Rand and L. Young (Springer, Berlin, 1981), Chap. 2, pp. 366–381.
- [19] H. Kantz and T. Schreiber, *Nonlinear Time Series Analysis* (Cambridge University Press, Cambridge, 2003).
- [20] R. A. York, A. Carreira-Rosario, L. M. Giocomo, and T. R. Clandinin, Flexible analysis of animal behavior via time-resolved manifold embedding, *bioRxiv* (2021), doi:10.1101/2020.09.30.321406.
- [21] T. D. Pereira, J. W. Shaevitz, and M. Murthy, Quantifying behavior to understand the brain, *Nat. Neurosci.* **23**, 1537 (2020).
- [22] T. Ahamed, A. C. Costa, and G. J. Stephens, Capturing the continuous complexity of behaviour in *Caenorhabditis elegans*, *Nat. Phys.* **17**, 275 (2021).
- [23] S. Tajima, T. Mita, D. J. Bakkum, H. Takahashi, and T. Toyozumi, Locally embedded presages of global network bursts, *Proc. Natl. Acad. Sci. USA* **114**, 9517 (2017).
- [24] S. R. Datta, D. J. Anderson, K. Branson, P. Perona, and A. Leifer, Computational neuroethology: A call to action, *Neuron* **104**, 11 (2019).
- [25] S. Strogatz, *Nonlinear Dynamics and Chaos: with Applications to Physics, Biology, Chemistry, and Engineering* (Westview Press, Boulder, 2015).
- [26] R. Payne and D. Webb, Orientation by means of long range acoustic signaling in baleen whales, *Ann. N.Y. Acad. Sci.* **188**, 110 (1971).
- [27] S. Fortune, S. Ferguson, A. Trites, B. LeBlanc, V. LeMay, J. Hudson, and M. Baumgartner, Seasonal diving and foraging behaviour of Eastern Canada–West Greenland bowhead whales, *Mar. Ecol. Prog. Ser.* **643**, 197 (2020).
- [28] K. Laidre, M. Heide-Jørgensen, and T. Nielsen, Role of the bowhead whale as a predator in West Greenland, *Mar. Ecol. Prog. Ser.* **346**, 285 (2007).
- [29] J. Citta, J. Olnes, S. Okkonen, L. Quakenbush, J. George, W. Maslowski, R. Osinski, and M. Heide-Jørgensen, Influence of oceanography on bowhead whale (*Balaena mysticetus*) foraging in the Chukchi Sea as inferred from animal-borne instrumentation, *Cont. Shelf Res.* **224**, 104434 (2021).
- [30] P. Priou, A. Nikolopoulos, H. Flores, R. Gradinger, E. Kunisch, C. Katlein, G. Castellani, T. Linders, J. Berge, J. A. Fisher *et al.*, Dense mesopelagic sound scattering layer and vertical segregation of pelagic organisms at the Arctic-Atlantic Gateway during the midnight sun, *Prog. Oceanogr.* **196**, 102611 (2021).
- [31] S. Gonzalez, J. K. Horne, and S. L. Danielson, Multi-scale temporal variability in biological-physical associations in the NE Chukchi Sea, *Polar Biology* **44**, 837 (2021).
- [32] P. G. H. Evans, Ecology and behaviour of the little auk *Alle alle* in West Greenland, *Ibis* **123**, 1 (1981).
- [33] K. M. Stafford, S. E. Moore, and C. G. Fox, Diel variation in blue whale calls recorded in the eastern tropical pacific, *Anim. Behav.* **69**, 951 (2005).
- [34] W. K. Oestreich, J. A. Fahlbusch, D. E. Cade, J. Calambokidis, T. Margolina, J. Joseph, A. S. Friedlaender, M. F. McKenna, A. K. Stimpert, B. L. Southall *et al.*, Animal-borne metrics enable acoustic detection of blue whale migration, *Curr. Biol.* **30**, 4773 (2020).
- [35] C. P. H. Elemans, W. Jiang, M. H. Jensen, H. Pichler, B. R. Mussman, J. Nattestad, M. Wahlberg, X. Zheng, Q. Xue, and W. T. Fitch, Evolutionary novelties underlie sound production in baleen whales, *Nature (London)* **627**, 123 (2024).
- [36] A. Pikovsky, M. Rosenblum, and J. Kurths, *Synchronization: A Universal Concept in Nonlinear Science* (Cambridge University Press, Cambridge, 2001).
- [37] S. Boccaletti, J. Kurths, G. Osipov, D. Valladares, and C. Zhou, The synchronization of chaotic systems, *Phys. Rep.* **366**, 1 (2002).
- [38] O. M. Tervo, M. F. Christoffersen, M. Simon, L. A. Miller, F. H. Jensen, S. E. Parks, and P. T. Madsen, High source levels and small active space of high-pitched song in bowhead whales (*Balaena mysticetus*), *PLoS ONE* **7**, e25072 (2012).
- [39] V. Senigaglia and H. Whitehead, Synchronous breathing by pilot whales, *Mar. Mammal Sci.* **28**, 213 (2012).
- [40] N. J. Quick, S. Isojunno, D. Sadykova, M. Bowers, D. P. Nowacek, and A. J. Read, Hidden Markov models reveal complexity in the diving behaviour of short-finned pilot whales, *Sci. Rep.* **7**, 45765 (2017).
- [41] B. Würsig and C. Clark, Behavior of bowhead whales, in *The Bowhead Whale*, edited by J. Burns, J. Montague, and C. Cowles (Allen Press, Lawrence, 1993), Chap. 5, pp. 157–199.
- [42] C. Clark, W. Ellison, and K. Beeman, Acoustic tracking of migrating bowhead whales, in *OCEANS '86* (IEEE, Washington, DC, USA, 1986), pp. 341–346.
- [43] K. Stafford and C. Clark, Acoustic behaviour, in *The Bowhead Whale: Balaena Mysticetus: Biology and Human Interactions*,

- edited by J. George and J. Thewissen (Academic Press/Elsevier, London, 2021), Chap. 22, pp. 323–338.
- [44] J. A. Fahlbusch, D. E. Cade, E. L. Hazen, M. L. Elliott, B. T. Saenz, J. A. Goldbogen, and J. Jahncke, Submesoscale coupling of krill and whales revealed by aggregative Lagrangian coherent structures, *Proc. R. Soc. B* **291**, 20232461 (2024).
- [45] H. M. Oliveira and L. V. Melo, Huygens synchronization of two clocks, *Sci. Rep.* **5**, 11548 (2015).
- [46] See Supplemental Material at <http://link.aps.org/supplemental/10.1103/PhysRevResearch.6.033174> for bowhead whale dive records from Disko Bay, West Greenland.
- [47] M. Heide-Jørgensen, R. Hansen, and O. Shpak, Distribution, migrations, and ecology of the Atlantic and the Okhotsk Sea populations, in *The Bowhead Whale: Balaena Mysticetus: Biology and Human Interactions*, edited by J. George and J. Thewissen (Academic Press/Elsevier, London, 2021), Chap. 5, pp. 57–75.
- [48] L. R. Nielsen, O. M. Tervo, S. B. Blackwell, M. P. Heide-Jørgensen, and S. Ditlevsen, Using quantile regression and relative entropy to assess the period of anomalous behavior of marine mammals following tagging, *Ecol. Evol.* **13**, e9967 (2023).
- [49] C. M. Albertsen, K. Whoriskey, D. Yurkowski, A. Nielsen, and J. M. Flemming, Fast fitting of non-Gaussian state-space models to animal movement data via template model builder, *Ecology* **96**, 2598 (2015).
- [50] E. Tan, S. Algar, D. Corrêa, M. Small, T. Stemler, and D. Walker, Selecting embedding delays: An overview of embedding techniques and a new method using persistent homology, *Chaos* **33**, 032101 (2023).